Contents lists available at ScienceDirect

Solid State Communications

Thermal dynamics of Au–Fe pair in silicon

Akbar Ali *, Abdul Majid

Advance Materials Physics Laboratory, Department of Physics, Quaid-i-Azam University, Islamabad, Pakistan

ARTICLE INFO

ABSTRACT

Deep level transient spectroscopy technique has been used to study the thermal dynamics of Au–Fe pairs in silicon during isochronal annealing. The formation and dissociation energies of an Au–Fe pair has been calculated by counting the number of pairs formed during each annealing. The respective energies of the Au–Fe pair are found to be ~ 0.36 eV and ~ 0.46 eV. The pairing of Au^- and Fe_i^+ takes place under predominant electrostatic forces.

© 2008 Elsevier Ltd. All rights reserved.

1. Introduction

Contamination by fast diffusion metal-impurities in silicon is a major yield-limiting factor in the sophisticated integrated ULSI/VLSI circuit technology [1–3]. Due to smaller device geometry and the increase in the number of transistors per chip, the impurities have become more important to be addressed [1]. Transition metals are well known to introduce point defects/complexes or precipitates in silicon; iron is the most common among them [1–13]. The presence of iron decreases the breakdown voltage of the gate oxides [3]. The electrical field breakdown failure is commonly reported to be caused by the formation of precipitates like pyramidal β-FeSi$_2$, rod-like α-FeSi$_2$, FeSi, γ-Fe$_2$O$_3$ and γ-FeSiO$_4$ [4–12]. Iron and other transition metals, in general, can occupy both the substitutional and tetrahedral interstitial sites that introduce multiple electronic states in the band gap [1–3]. The conversion of the defects from substitutional to interstitial sites during quenching can significantly affect the electronically driven defect reactions [3, 13,14] in the base material, silicon, used for the device fabrication. Pairing of interstitial iron with shallow dopants (Fe–P, Fe–B, Fe–A, Fe–Ga, Fe–In and Fe–Ti), transition metals (Fe–Au, Fe–Ag, Fe–Pd, Fe–Pt and Fe–Zn) and other impurities (FeS, FOV etc) is well documented [3]. A lot of work has been done on such systems and their reactions but there are many corners still left unexplored.

The study of iron related defects in order to understand the mechanism of transformation reaction from one type of defect to another has not yet lost its significance. Au–Fe complex is one that still has much attraction for scientists [1–3]. Significantly different values of formation and dissociation energies of this complex and many possibilities of accounting for the difference are reported [2, 16–18]. The nature of the bonding of the pair, whether covalent or ionic, is still an unanswered question. Here we report the thermal dynamics of the pairing reaction $\{Au^- + Fe_i^+ = Fe_i^+ - Au^-\}$ of Au–Fe, which is part of an ongoing project on the complexes of iron and other transition metals in silicon.

2. Experimental

The p$^+$n junctions of silicon encapsulated in a quartz tube (evacuated and then filled with Argon gas at atmospheric pressure) after standard etching and cleaning were heat treated at 950 °C followed by quenching in water. Ohmic contacts were made on the back surface by rubbing gallium with an aluminum rod. The shallow doping concentration (phosphorus) found from C–V characteristics was $\sim 10^{14}$ cm^{-3}. Untreated samples were taken as reference. After selecting suitable diodes, deep level transient spectroscopy technique (DLTS) [19] has been employed to study the thermal dynamics of the Au–Fe complex. Typical DLTS scans S1 and S3 of the virgin and annealed samples, respectively, are shown in Fig. 1. The inset shows the DLTS signal due to the Au–Fe complex. The peaks appearing in the spectra are marked with the activation energies of the corresponding defects. The activation energies of Au and the Au–Fe complex measured from emission rate data [20] are Ec–0.55 eV and Ec–0.34 eV, respectively.
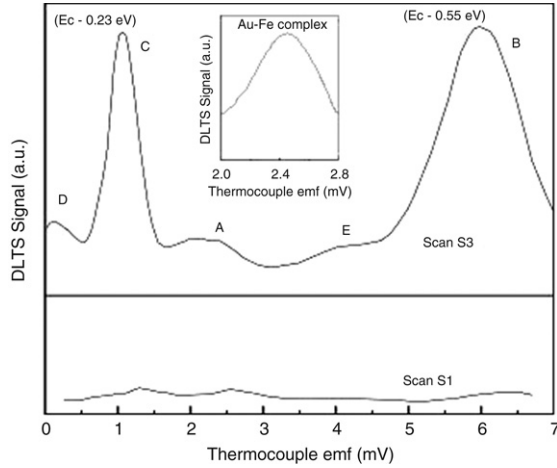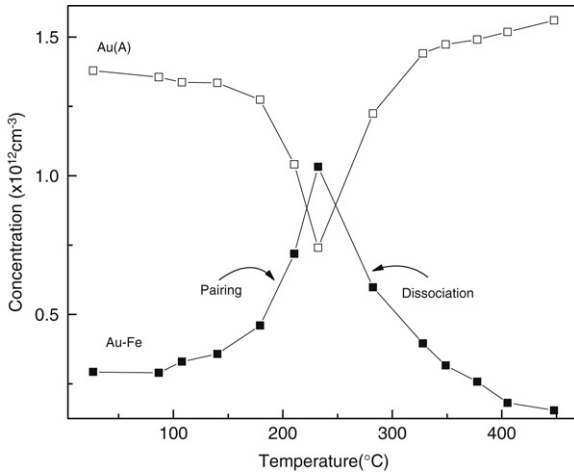
Fig. 1. DLTS scans of reference and quenched silicon samples.

Fig. 2. Annealing characteristics of Au(A) and Au–Fe complex.

Annealing of the samples was performed in nitrogen ambient up to ∼450 °C. The samples were heated each time at a fixed temperature for ∼25 min under a continuous flow of nitrogen gas. To study the response of the Au–Fe complex (pairing and dissociation reaction) to the annealing temperature, the DLTS scans were taken under identical conditions immediately after pulling the samples out from the furnace. The concentration of the complex has been calculated from the respective peak heights [19]. The annealing characteristics of both gold and the Au–Fe complex are given in Fig. 2.

3. Results

Our objectives here are to measure the pairing and dissociation energies of the Au–Fe complex, therefore DLTS scans and thermal characteristics of Au(A) and the Au–Fe complex reported earlier [20] have been given here only for sake of completeness. During annealing a DLTS peak (shown in the inset of Fig. 1) appears which is identified as the Au–Fe complex at energy position $E_c -$ 0.34 eV within the band gap of silicon [20]. Gold and iron have not been deliberately doped but are present in the as-grown samples, having occupied electrically active or inactive sites (precipitates) that migrate to active sites on heating. The constituents of the Au–Fe pair are substitutional gold (acceptor) and interstitial iron (donor) (Fe$_i$ + Au$_s$ = Au–Fe) [21,22]. The fraction of iron atoms involved in the reaction and pairing time constant can be
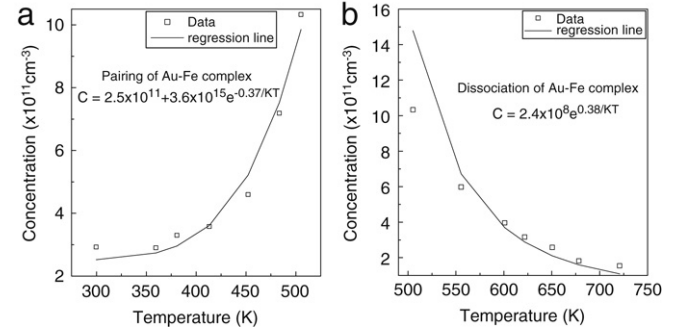

Fig. 3. (a) Pairing (b) Dissociation reaction of Au–Fe complex. The solid line shows the best fit exponential by hit and trial method passing through the data points.
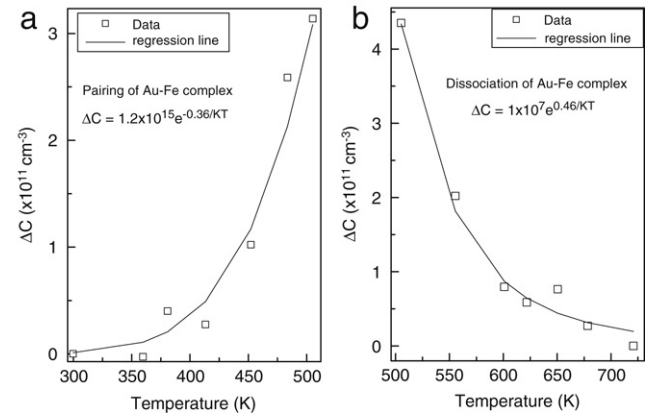

Fig. 4. Reaction showing (a) pairing (b) dissociation of the fraction of the Au–Fe complex. The solid line shows best fit exponential by hit and trial method passing through the data points.

correlated by the following Eqs. [16,18]:

$$[\text{Au–Fe}_i]/\{[\text{Au}][\text{Fe}_i]\} = \{[\text{Au}]/ZN\}\{\exp(\Delta S/k)\exp(\Delta H/kT)\} \quad (1)$$

$$\tau = \varepsilon KT/\{4\pi q^2 D(\text{Fe}_i)[\text{Au}_s]\} = 557T/\{D(\text{Fe}i)[\text{Au}_s]\} \quad (2)$$

where [Au], [Au–Fe$_i$] are respective concentrations, N is the number of lattice sites per cm^3, Z is the number of pair configurations about one site and $D(\text{Fe}_i) = 0.33\exp(-0.81/KT)$ [16,18].

The above equation is further simplified, as given below, to calculate the pairing and dissociation energies of the Au$_s$–Fe$_i$ pair.

$$[\text{Au–Fe}_i] = C_\circ \exp(E/KT) \quad (3)$$

where, $C_\circ$ contains Z, N, [Au], [Fe$_i$] and the entropy term etc.

The data have been arranged into two different categories as case 1 and case 2. Two slightly different methods have been adopted to calculate the energy of the pair formation.

Case 1: Total concentration of the Au–Fe pair existing after each annealing is considered for calculation.

Case 2: The fractional change (increase or decrease) in concentration of the Au–Fe pair during annealing is accounted for the calculation of pairing or dissociation energies.

Method 1: A suitable exponential fitted through the data points has been guessed using a statistical program available in the computer software. After finding such an exponential the parameters are adjusted by a hit and trial method to fit the data points by changing the values of amplitude ($C_\circ$) and energy (E).

Method 2: The data has been plotted on a monolog graph and a regression line is fitted through the data points. The energy has been calculated from the slope of the line.

The pairing and dissociation energies estimated by method 1 for case 1 have been found as 0.37 eV and 0.38 eV {Fig. 3(a) and (b)},
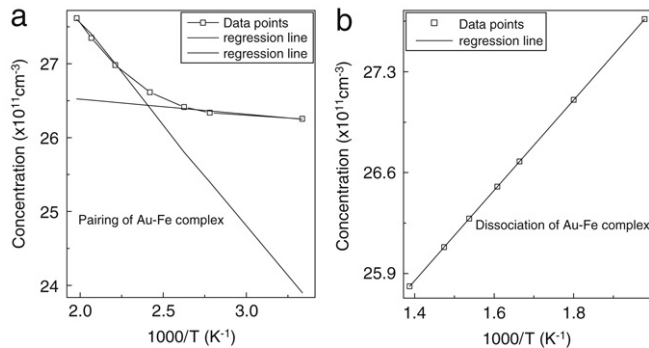
Fig. 5. Monolog plot of (a) pairing (b) dissociation reactions of Au–Fe complex. The solid line is best fit regression line.
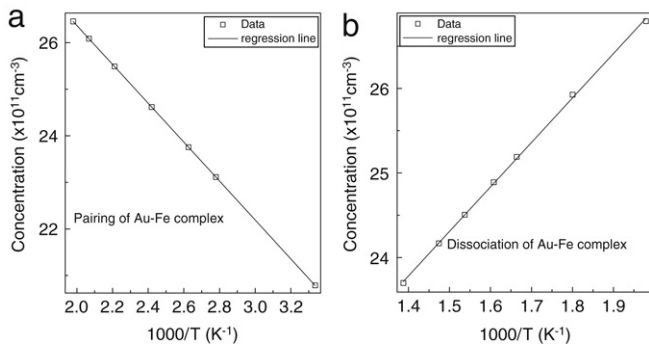

Fig. 6. Monolog plot of (a) pairing (b) dissociation reactions of fraction of Au–Fe complex. The solid line is best fit regression line.

Fig. 7. Rate of (a) formation (b) dissociation of the Fe- Au pair.

respectively. Similarly for case 2 {Fig. 4(a) and (b)} the respective values of the energies once again were calculated as about 0.36 eV and 0.46 eV.

A single line was not found to fit through all the data points of the pairing reaction for case 1 by method 2, therefore, two different lines have been fitted; one for the slower and second for the faster parts of the reaction{Fig. 5(a)}. The respective pairing energies for the slower and faster parts were found about 0.02 eV and 0.20 eV. On the other hand a single regression line was found fit properly {Fig. 5(b)} through the data points for dissociation reaction that yielded the energy to be 0.27 eV. The pairing and dissociation energies once again were calculated for case 2 using method 2. In this case a single line fits through the data points for both the pairing {Fig. 6(b)} and dissociation {Fig. 6(b)} reactions. The respective energies were found to be 0.36 eV and 0.45 eV.

It is strange to note that a difference in evaluation technique affects the values of energies drastically for case 1. The same value of energies of pairing and dissociation reactions, calculated by both methods for case 2, points to the fact that instead of total concentration, the fraction of concentration involved in a reaction gives more precise values of the energies.

The semi log plots (Fig. 7(a), (b)) show that $1/\tau = 2 \times 10^6 \exp(-0.85/KT)$ and $1/\tau = 559 \exp(-0.47/kT)$ fit best through the data points measured for the association and dissociation reactions of the Au–Fe complex with the energies of pair formation and dissociation 0.85 eV and 0.47 eV, respectively. The energy for dissociation reaction is again very close to the value calculated above but for pairing reaction it is different. The energy of pair formation is nearly the same as that reported for an iron–boron pair (a carrier emission limited process) [16]. The pre-exponential factor for the dissociation reaction is much smaller than that of pairing of the Au–Fe complex. The exponentials are fitted through the data for pairing and dissociation reactions, pre-exponential factors and pairing/dissociation energies are also given in Table 1 for comparison.
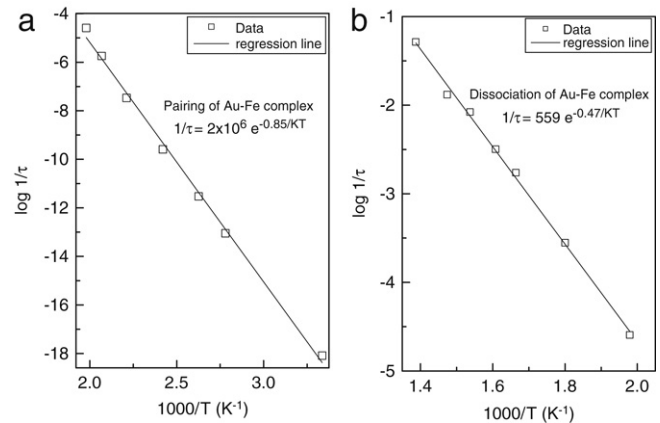
4. Discussion

The complexes of gold and 3d transition metals, especially of gold and iron, in silicon remained a hot topic since the pioneering work of Collins and Carlson [25]. During the study of iron gold complexes an electron emitting level at $E_c - 0.33$ eV [24–28] and $E_c - 0.34$ eV [20] was identified as an iron-gold pair. The activation energy for migration of iron atoms in silicon is reported to be 0.85 eV and 0.82 eV [16,8]. The binding energy of the Au–Fe complex has been estimated by different workers to be 0.9 eV [17], 0.68 eV [2] and 1.22 eV [16,18]. The activation energy calculated from the slope of the data measured for the diffusion coefficient of iron in silicon at different temperatures was found to be 0.44 eV [16,18]. Many possibilities have been discussed to account for this difference but a final conclusion could not be arrived at to propose a suitable model for the Au–Fe complex [3,18].

A theoretical model based on the ionic model of Ludwig and Woodbury [15] was proposed by Kleinhenz et al. [29] and Severt et al. [30] to account for the EPR signal coming from magnetic coupling between the angular momenta of gold and iron. The transfer of one electron from iron to gold due to higher electronegativity of the gold as compared to iron was speculated to make the $Fe_i^+ Au_s^-$ centre [29]. The strong magnetic coupling between Au_s^- ($S = 1$) and Fe_i^+ ($S = 3/2$) was assumed to be responsible for the effective spin of $S = 1/2$.

Asali et al. [31,32] proposed a different model based on covalent interaction including silicon neighbors in addition to Fe_i^+ and Au_s^-. By simulating over a cluster of 25 silicon atoms they showed that spin $S = 1/2$ is related to molecular orbital spread out over the cluster. He also proposed the covalent bonding energy of the pair as about 1.2 eV. Overhof and Weihrich [33] predicted the energies for trigonal $(Au_sFe_i)^{0/+}$ and $(Au_sFe_i)^{-/0}$ to be $E_v + 0.45$ eV and $E_c - 0.35$ eV, respectively, which are in good agreement with experimentally measured values [10,23]. They also predicted the covalent bonding energy of the pair as about 1.2 eV and suggested that an Fe–Au pair in arthorhombic symmetry has 0.3 eV lower binding energy than a trigonal pair. Lemky [34] and Brotherton et al. [18] studied the pairing reaction and reported binding energy of the complex to be 0.75 eV and 1.22 eV, respectively, for the Fe–Au complex. Istratov et al. [3] emphasized that the difference in energies, reported by both the groups, stems from the different interpretations of the experimental data rather than the difference in the measured data-points themselves. The data are in reasonably good agreement with each other when the ratio of the pair concentration and the product of individual concentrations taken from the data of both the two groups are plotted together. Although Istratov et al. [3] tried to sort out the difference in binding energies,

Table 1
Pairing and dissociation energies and exponentials fitted through pairing and dissociation reaction data by hit and trial method

Method	Type of data	Exponentials fitted		Energy (eV)	
		Pairing	Dissociation	Pairing	Dissociation
1	1	$C = 2.5 \times 10^{11} + 3.6 \times 10^{15} \exp(-0.37/kT)$	$C = 6 \times 10^7 \exp(0.38/kT)$	0.37	0.38
	2	$\Delta C = 1.2 \times 10^{15} \exp(-0.36/kT)$	$\Delta C = 1 \times 10^7 \exp(0.46/kT)$	0.36	0.46
2	1	–	–	0.24 (faster part)	0.27
		–	–	0.02 (slower part)	
	2	–	–	0.36	0.45
	1	$1/\tau = 2 \times 10^6 \exp(-0.85/kT)$	$1/\tau = 559 \exp(-0.47/kT)$	0.85	0.47

the nature of pairing whether covalent or ionic still remained unresolved.

In our samples iron atoms are supposed to be present inadvertently on electrically inactive sites, maybe as precipitates, and the diffusion process has been assumed to have been completed already. We performed annealing of the samples and calculated the energy of formation using the above equations without taking into account the entropy component. The energies calculated for different cases and methods for pairing of Au–Fe are 0.37 eV, 0.36 eV, 0.24 eV and 0.36 eV. Similarly the dissociation energies are found to be 0.38 eV, 0.46 eV, 0.27 eV, 0.45 eV. Ignoring the values of energy calculated for case 2 of the Au–Fe pairs the average values come to be 0.36 eV and 0.43 eV, respectively, for the pairing and dissociation reactions but, in our opinion, the values calculated by method 2 for the data, type 2, are the most appropriate because in that case the actual number of Au–Fe pairs produced during each annealing has been incorporated. The higher value of dissociation energy as compared to the pairing of the gold–iron pair suggests that Au–Fe is a stable complex at room temperature, once it is formed at some higher temperature. The dissociation of the pair has been assumed to proceed by a two stage process. In the second stage precipitation of iron from electrically active lattice sites is suggested, which is also thought to be responsible for the irreversibility of the reaction [16, 18]. The energies calculated for case 1 by method 2 appear to be misleading because the calculation includes the pair already formed, which doesn't participate in the reaction taking place at that specific temperature. However the values of pairing energies for slower (0.02 eV) and faster (0.24 eV) parts indicate that at a lower temperature the reaction is very slow. The low values can be justified by assuming (1) the possibility of a fraction of the complex formed by covalent bonding at slightly above room temperature, where a very minor energy is required by an iron atom to move closer to a substitutional Au atom to form a covalent pair, or (2) the equilibrium concentrations of the pair (Fe^+ and Au^- ions) might not have been achieved at a lower temperature, which lead to the slow kinetics of the reaction.

The lattice vibration (phonon) frequency at room temperature is about $\sim 10^{12} - 10^{13} \, s^{-1}$, and the pre-exponential factor in the time constant equation, mentioned in Table 1, suggest that the energy associated with lattice vibration is sufficient for a single jump from an unpaired to a paired state [24] and the reaction kinetics should not be slow. Therefore, the pair formation process is not rate limited and rules out the possibility of pairing between neutral atoms by covalent bonding. Option 2 is the only suitable candidate to explain the slower kinetics of the reaction at lower temperatures. The only possibility that can be addressed now is the pairing between Au^- and Fe_i^+ under predominantly electrostatic forces. If the pairing energy 0.36 eV is added to the activation energy 0.82 eV reported for iron precipitation in non gold doped silicon, the sum is very close to the reported value 1.2 eV [18], which suggests that at a higher temperature pairing reaction is driven by the opposite polarities of the building constituents, gold acceptor and iron donor atoms in the case of the Fe–Au pair/complex. Thermal energy at elevated temperatures helps only

migration of iron atoms. When iron atoms approach the effective capture radius $R\{R = \{\int (dr/r^2) \exp[V(r)/Kt]\}^{-1}$ of gold atoms [due to attractive interaction energy V(r)] between gold acceptor (negatively charged) and iron donor atoms (positively charged)} they are captured by gold atoms, which results in the formation of the iron gold-complex. This model for the formation of the Au–Fe complex can also be supported by the following observations.

Iron–boron pairs in p-type samples have been observed to be formed within a couple of days at room temperature [13] and if the diffusion of iron is a rate limiting process, the time constant for Au–Fe pairing would not be greater than four to five times that of iron–boron pairing [16,18]. The pairing of the Au–Fe complex in silicon at room temperature has not been observed to be formed even in one month's storage time [23]. Therefore the absence of a noticeable pairing of Au–Fe at room temperature suggests that the pairing of Au and Fe is between charge impurities driven by electrostatic attraction between Fe_i^+ and Au_s^- [16,18]. The low pre-exponential factors calculated for dissociation (much less than the lattice phonon vibration frequency) by both the above methods suggest that dissociation of the Au–Fe pair is a carrier emission limited process.

Electrostatic pair binding energy (0.85 eV) calculated from the time constant equation $\{1/\tau = 2 \times 10^6 \exp(-0.85/KT)\}$, rather than the reported value, is similar to that calculated by Kimerling et al. [16,18] for the iron boron pair in silicon.

The dissociation energy $1/\tau_{diss} = 559 \exp(-0.47/kT)$ is less than the reported value $\tau_{diss} = 4.7 \times 10^{-3} \exp(-0.73/kT)$ [35]. The difference comes from the diffusion barrier which is not included in our case.

Acknowledgement

References

[1] A.A. Istratov, H. Hieslmair, E.R. Weber, Appl. Phys. A 70 (2000) 489.
[2] Eicke R. Weber, Appl. Phys. A 30 (1) (1983).
[3] A.A. Istratov, H. Hieslmair, E.R. Weber, Appl. Phys. A 69 (13) (1999).
[4] W. Schröter, M. Seibt, D. Gilles, in: R.W. Cahn, P. Haasen, E.J. Kramer (Eds.), Materials Science and Technology: A Comprehensive Treatment, VCH, New York, 1991, p. 576.
[5] M. Ronay, R.G. Schad, Phys. Rev. Lett. 64 (1990) 2042.
[6] J. Wong-Leung, D.J. Eaglesham, J. Sapjeta, D.C. Jacobson, J.M. Poate, J.S. Williams, J. Appl. Phys. 83 (1998) 580.
[7] K. Honda, A. Ohsawa, T. Nakanishi, J. Electrochem. Soc. 142 (1995) 3486.
[8] K. Honda, T. Nakanishi, A.W. Ohsawa, N. Toyokura, J. Appl. Phys. 62 (1987) 1960.
[9] N. Nishio, T. Taketomi, M. Morita, S. Ohi, H. Mikoshiba, in: J.L. Benton, G.N. Maracas, P. Rai-Choudhury (Eds.), Diagnostic Techniques for Semiconductor Materials and Devices, The Electrochem. Soc, Pennington, 1992, p. 164.
[10] A.G. Cullis, L.E. Katz, Philos. Mag. 30 (1974) 1419.
[11] H. Mikoshiba, N. Nishio, T. Matsumoto, H. Kikuchi, T. Kitano, H. Kaneko, in: S. Ashok, J. Chevallier, K. Sumino, E. Weber (Eds.), Defect Engineering in Semiconductor Growth, Processing and Device Technology, Mater. Res. Soc, Pittsburgh, 1992, p. 629.
[12] S. Sadamitsu, A. Sasaki, M. Hourai, S. Sumita, N. Fujino, Jpn. J. Appl. Phys. 30 (1991) 1591.
[13] Daniel Macdonald, L.J. Geerligs, Appl. Phys. Lett. 85 (2004) 4061.

[14] J.D. Gerson, L.J. Cheng, J.W. Corbett, J. Appl. Phys. 48 (1977) 4821.
[15] G.W. Ludwig, H.H. Woodbury, Solid State Phys. 13 (1962) 223.
[16] L.C. Kimerling, J.L. Benton, Physica B 116 (1983) 297;
S.D. Brotherton, P. Bradley, A. Gill, J. Appl. Phys. 57 (1985) 1783.
[17] H. Lemke, Phys. Status Solidi A 75 (1983) 473.
[18] H. Nakashima, T. Isobe, Y. Yamamoto, K. Hashimoto, Jpn. J. Appl. Phys. 27 (1988) 1542;
T. Isobe, H. Nakashima, K. Hashimoto, Jpn. J. Appl. Phys. 28 (1989) 1282.
[19] D.V. Lang, J. Appl. Phys. 45 (1974) 3023.
[20] Akbar Ali, Abdul Majid, J. Mater. Sci. 42 (2007) 4753;
Akbar Ali, M. Zafar Iqbal, N. Baber, Asghar Ali Gil, Semicond. Sci. Technol. 11 (1996) 129.
[21] Shuji Tanaka, Hajime Kitagawa, Jpn. J. Appl. Phys. 37 (1998) 4656; 34 (1995) L 721.
[22] L.V.C. Assali, J.R. Leite, A. Fazzio, Phys. Rev. B 32 (1985) 8085.
[23] Akbar Ali, U.S. Qurashi, M. Zafar Iqbal, N. Zafar, Semicond. Sci. Technol. 12 (1997) 1100.

[24] A. Mesli, T. Heiser, Phys. Rev. B 45 (1992) 11632.
[25] C.B Collins, R.O Carlson, Phys. Rev. 108 (1957) 1409.
[26] H. Feichtinger, Inst. Phys. Conf. Ser. 46 (1979) 528.
[27] E.R. Weber, in: R.B. Fair, C.W. Pearce, J. Washburn (Eds.), Impurity Diffusion and Gettering in Silicon, Mater. Res. Soc, Pittsburghh, PA, USA, 1985, p. 3.
[28] Y.H. Lee, R.L. Kleinhenz, J.W. Corbett, Inst. Phys. Conf. Ser. 46 (1979) 521.
[29] R.L. Kleinhenz, Y.H. Lee, J.W. Corbett, E.G. Sieverts, S.H. Muller, C.A.J. Ammerlaan, Phys. Status Solidi B 108 (1981) 363.
[30] E.G. Sieverts, S.H. Muller, C.A.J. Ammerlaan, R.L. Kleinhenz, J.W. Corbett, Phys. Status Solidi B 109 (1982) 83.
[31] L.V.C. Assali, J.R. Leite, A. Fazzio, Phys. Rev. B 32 (1985) 8085.
[32] L.V. Assali, J.F. Justo, Phys. Rev. B 58 (1998) 3870.
[33] H. Overhof, H. Weihrich, Phys. Rev. B 55 (1997) 10508. 287;
H. Overhof, H. Weihrich, Mater. Sci. Forum 196– 201 (1995) 1357.
[34] H. Lemke, Phys. Status Solidi A 75 (1983) 473.
[35] E.R. Weber, N. Wiehl, in: S. Mahajan, J.W. Corbett (Eds.), Defects in Semiconductors II, North-Holland, New York, 1983, p. 19.